

## Comparison of Integral Equation Formulations for Stokesian Particulate Flow Simulations

Gökberk Kabacaoğlu 

Bilkent University, Faculty of Engineering, Department of Mechanical Engineering, Ankara, Türkiye,  
gkabacaoglu@bilkent.edu.tr

### ARTICLE INFO

### ABSTRACT

Keywords:  
Stokes flow  
Green's function  
Boundary integral equations  
Suspensions  
Stability



#### Article History:

Received: 15.08.2024

Revised: 16.12.2024

Accepted: 16.01.2025

Online Available: 12.02.2025

Particulate Stokesian flows describe the hydrodynamics of rigid or deformable particles within Stokes flows, where viscous forces dominate over inertial effects. These flows are characterized by highly nonlinear fluid-structure interactions, moving interfaces, and multiple spatial and temporal scales, making numerical simulations both complex and computationally expensive. Accurately capturing these interactions requires sophisticated numerical approaches. The boundary integral equation method (BIEM) is a powerful tool for modeling such flows, as it reduces computational complexity by limiting the discretization to the immersed particle boundaries rather than the entire flow domain. This efficiency makes BIEM particularly suitable for studying systems with many particles or complex boundary geometries. In this work, we explore two fundamental BIEM formulations for Stokesian flows involving rigid particles: the first-kind and second-kind integral equations. These formulations differ in their mathematical structure and computational properties, impacting their stability, accuracy, and overall performance. By comparing these two approaches, we aim to highlight their respective advantages and limitations, providing insights into their applicability to different particulate flow scenarios. This analysis contributes to the broader understanding of numerical methods for Stokesian flows, addressing challenges inherent to fluid-structure interactions and advancing computational techniques in this field.

## 1. Introduction

Stokesian particulate flows are the flows of a collection of rigid or deformable particles (e.g., drops, capsules, cells, slender bodies, and filaments, possibly elastic or filled by a fluid) that are suspended in a Newtonian fluid and the particle Reynolds number is vanishingly small [1-3]. The hydrodynamics of colloidal suspensions of passive particles is a well-established but still active area of research in soft condensed matter physics and chemical engineering. Recently, there has been growing interest in suspensions of active colloids, which display rich collective behaviors that are quite different from those of passive suspensions [4-7].

The number of computational methods for modeling active suspensions has been increasing,

often building on well-established techniques used for passive suspensions in steady Stokes flow, which occurs at zero Reynolds number [8-10]. Since active particles often contain metallic components, they are typically much denser than the solvent, causing them to sediment towards the bottom wall. This necessitates addressing confinement and implementing nonperiodic boundary conditions in any simulation method aimed at experimentally relevant scenarios.

Additionally, because the collective motions observed in active suspensions involve large numbers of particles and hydrodynamic interactions among particles decay slowly with distance, it is essential to develop methods that can capture long-range hydrodynamic effects while still scaling to tens or hundreds of thousands of particles [11].

A computational method for colloidal suspensions must incorporate two essential components: long-range hydrodynamic interactions and the correlated Brownian motion of the particles. When active and Brownian motion are not present, accurately describing the hydrodynamics of Stokesian suspensions involves solving mobility problems [12]. This requires calculating the linear and angular velocities of the particles in response to applied external forces and torques. For deterministic Stokes problems, the Boundary Integral Method (BIM) [13] is a highly developed technique that effectively manages complex particle shapes and ensures controlled accuracy, even in dense suspensions. In this approach, the steady Stokes equations are reformulated as an integral equation with unknown densities defined on the boundary, using either a first kind (single-layer densities) or second kind (double-layer densities) formulation, or a combination of both [14-16].

Particles with intricate geometries can be directly discretized using a surface mesh, and with an appropriate choice of surface quadrature, higher-order (or even spectral) accuracy can be attained. The main challenge lies in addressing the singularity of the Green's functions that arise in the boundary integral formulation [17]. Discretizing the boundary integral equation typically results in a dense linear system, necessitating the use of fast algorithms, such as the Fast Multipole Method (FMM) [14], to efficiently perform the dense matrix-vector product and achieve linear scaling. In this study, we aim at comparing the first kind formulation with the second kind formulations. One of such second kind formulations is Power & Miranda's formulation [18]. In addition to that, we suggest another symmetric formulation. The comparison is based on the stability and accuracy of the methods in two dimensions.

## 2. General Methods

Here we mostly follow the notation in [19]. We consider a suspension of  $M$  rigid bodies  $\{\mathcal{B}\}_{p=1}^M$ , with tracking points  $\mathbf{q}_p$  and orientations  $\theta_p$ ; in compact form  $\mathbf{x}_p = \{\mathbf{q}_p, \theta_p\}$ . We denote the linear and angular velocity by  $\mathbf{u}_p$  and  $\omega_p$ , respectively. The force and the torque on

the body are shown with  $\mathbf{f}_p$  and  $\tau_p$ . In compact notation,  $\mathbf{F}_p = \{\mathbf{f}_p, \tau_p\}$  and  $\mathbf{U}_p = \{\mathbf{u}_p, \omega_p\}$ . Vectors without scripts refer to the composite vector formed by the variables of all the bodies, i.e.,  $\mathbf{U} = \{\mathbf{U}_p\}_{p=1}^M$ . We define a block diagonal geometric operator,  $\mathcal{K} = \{\mathcal{K}_p\}_{p=1}^M$ , that transforms rigid body velocities into surface velocities

$$\mathcal{K}[\mathbf{U}](\mathbf{x}) = \mathbf{u}_p + \omega_p(\mathbf{x} - \mathbf{q}_p)^\perp \text{ for } \mathbf{x} \in \partial\mathcal{B}_p \quad (1)$$

where  $\mathbf{x}^\perp = (x_2, -x_1)$ . The adjoint of  $\mathcal{K}$  integrates the surface traction of the bodies and yields the total external force and torque on the bodies

$$\begin{aligned} \mathcal{K}^* \boldsymbol{\lambda} &= \mathbf{F} \\ &= \left\{ \left[ \begin{array}{c} \int \boldsymbol{\lambda}(\mathbf{x}) d\mathcal{B}_p \\ \int (\mathbf{x} - \mathbf{q}_p)^\perp \cdot \boldsymbol{\lambda}(\mathbf{x}) d\mathcal{B}_p \end{array} \right]_p \right\}_{p=1}^M. \end{aligned} \quad (2)$$

The operators  $\mathcal{K}$  and  $\mathcal{K}^*$  are adjoint. For an arbitrary function defined on the surface of the bodies,  $\mathbf{g}(\mathbf{x})$ , and a collection of vectors defined on the bodies,  $\mathbf{U}$ , these operators satisfy

$$\begin{aligned} (\mathbf{g}, \mathcal{K}[\mathbf{U}]) &= \int \mathbf{g}(\mathbf{x}) \cdot \mathcal{K}[\mathbf{U}](\mathbf{x}) d\mathcal{B} \\ &= (\mathcal{K}^* \mathbf{g}) \cdot \mathbf{U}. \end{aligned} \quad (3)$$

Flows of rigid bodies in the limit of vanishing Reynolds numbers (i.e., the ratio of inertial forces to the viscous forces is zero) are governed by the Stokes equations

$$-\nabla p + \eta \nabla^2 \mathbf{v} = 0 \quad (4)$$

$$\nabla \cdot \mathbf{v} = 0 \quad (5)$$

where  $p$  is fluid pressure,  $\eta$  is fluid viscosity and  $\mathbf{v}$  is fluid velocity. The Green's functions for the Stokes equations are the so-called Stokeslet and stresslet. We consider a two-dimensional problem. The Stokeslet is

$$G_{ij}(\mathbf{x}, \mathbf{y}) = G_{ij}(\mathbf{r}) = \frac{1}{4\pi\eta} \left( -\delta_{ij} \log r + \frac{r_i r_j}{r^2} \right) \quad (6)$$

where  $\mathbf{r} = \mathbf{x} - \mathbf{y}$  and  $r = |\mathbf{r}|_2$ . The stresslet is

$$T_{ijk}(\mathbf{x}, \mathbf{y}) = T_{ijk}(\mathbf{r}) = -\frac{1}{\pi} \frac{r_i r_j r_k}{r^4} \quad (7)$$

The single layer, the double layer and the adjoint double layer operators acting on an arbitrary function  $\mathbf{g}(\mathbf{x})$  on a body surface are defined as

$$(\mathcal{S}[\mathbf{g}])_i(\mathbf{x}) = \mathcal{S}_i[\mathbf{g}] = \int G_{ij}(\mathbf{x}, \mathbf{y}) g_j(\mathbf{y}) d\mathcal{B} \quad (8)$$

$$(\mathcal{D}[\mathbf{g}])_i(\mathbf{x}) = \mathcal{D}_i[\mathbf{g}] = \int T_{ijk}(\mathbf{x}, \mathbf{y}) n_k(\mathbf{y}) g_j(\mathbf{y}) d\mathcal{B} \quad (9)$$

$$(\mathcal{D}^*[\mathbf{g}])_i(\mathbf{x}) = \mathcal{D}_i^*[\mathbf{g}] = -n_k(\mathbf{x}) \int T_{ijk}(\mathbf{x}, \mathbf{y}) g_j(\mathbf{y}) d\mathcal{B} \quad (10)$$

where  $\mathbf{n}$  is the surface normal pointing into the fluid. The last two double layer operators are adjoint, i.e., for any functions  $\mathbf{g}$  and  $\mathbf{h}$

$$(\mathbf{g}, \mathcal{D}[\mathbf{h}]) = (\mathcal{D}^*[\mathbf{g}], \mathbf{h}). \quad (11)$$

### 2.1. First kind formulation

Now, let us complete the continuous formulation for flows rigid particles. As mentioned above, the fluid flow is governed by the Stokes equations. The fluid satisfies the no-slip boundary condition on the bodies

$$\mathbf{v}(\mathbf{x}) = \mathcal{K}[\mathbf{U}](\mathbf{x}) \text{ for } \mathbf{x} \in \partial\mathcal{B} \quad (12)$$

If  $-\boldsymbol{\lambda}$  is the fluid traction on the bodies, the force-torque balance leads to

$$\mathcal{K}^* \boldsymbol{\lambda} = \mathbf{F}. \quad (13)$$

Let  $\mathbf{u}_\infty$  be the background flow moving the particles. With these equations, we can write the first-kind formulation that leads to a symmetric, positive-definite matrix in the linear system to be solved for the traction and rigid body velocity:

$$\begin{bmatrix} \mathcal{S} & -\mathcal{K} \\ -\mathcal{K}^* & 0 \end{bmatrix} \begin{bmatrix} \boldsymbol{\lambda} \\ \mathbf{U} \end{bmatrix} = \begin{bmatrix} \mathbf{u}_\infty \\ -\mathbf{F} \end{bmatrix}. \quad (14)$$

### 2.2. Second kind formulation

Second kind formulation involves the double layer integral which has better conditioning than the single layer integral. One alternative for the second kind formulation is as follows. According to Pozrikidis [13], the no-slip boundary condition can be written as

$$\frac{1}{2} \mathcal{K}[\mathbf{U}] + \mathcal{D}(\mathcal{K}[\mathbf{U}]) + \mathbf{u}_\infty = \mathcal{S}[\boldsymbol{\lambda}](\mathbf{x}) \quad (15)$$

The force-torque balance on the bodies can be written as

$$\frac{1}{2} \mathcal{K}^* \boldsymbol{\lambda} + \mathcal{K}^* \mathcal{D}^*[\boldsymbol{\lambda}] = \mathbf{F}. \quad (16)$$

These equations form a linear system for the traction and rigid body velocities

$$\begin{bmatrix} \mathcal{S} & -\frac{1}{2} \mathcal{K} - \mathcal{D}\mathcal{K} \\ -\frac{1}{2} \mathcal{K}^* - \mathcal{K}^* \mathcal{D}^* & 0 \end{bmatrix} \begin{bmatrix} \boldsymbol{\lambda} \\ \mathbf{U} \end{bmatrix} = \begin{bmatrix} \mathbf{u}_\infty \\ -\mathbf{F} \end{bmatrix}. \quad (17)$$

The fact that this first alternative has the single layer operator on the diagonal, its conditioning is determined mostly by the single layer operator. Another alternative can be

$$\begin{bmatrix} \mathcal{S} + \frac{1}{\eta}(-I + \mathcal{D} + \mathcal{D}^*) & -\mathcal{K} \\ -\mathcal{K}^* & 0 \end{bmatrix} \begin{bmatrix} \boldsymbol{\lambda} \\ \mathbf{U} \end{bmatrix} = \begin{bmatrix} \mathbf{u}_\infty \\ -\mathbf{F} \end{bmatrix}. \quad (18)$$

The proof is as follows. An arbitrary flow on a surface  $\mathcal{L}$  surrounding a particle  $\mathcal{B}$  but far from the particle can be written as [20]

$$\mathbf{v}(\mathbf{x}) = \left( \mathcal{S} + \frac{1}{\eta}[\mathcal{D} + \mathcal{D}^*] \right) [\boldsymbol{\lambda}](\mathbf{x}) \text{ for } \mathbf{x} \in \mathcal{L}. \quad (19)$$

When the surface  $\mathcal{L}$  approaches to the particle surface, we get

$$\mathbf{v}(\mathbf{x}) = \left( \mathcal{S} + \frac{1}{\eta}[-I + \mathcal{D}^{P.V.} + (\mathcal{D}^*)^{P.V.}] \right) [\boldsymbol{\lambda}](\mathbf{x}) \text{ for } \mathbf{x} \in \mathcal{B}. \quad (20)$$

The integrals are in the principal value sense.

### 2.3. Confined flow

In confined flows, the confining boundary induces flow on the particles. To maintain the symmetry properties of the linear system, we write an integral equation for the outer boundary using the same second kind formulation used for the rigid body. Let us introduce operators for the interaction between the outer boundary (denoted with subscript  $o$ ) and the rigid body (denoted with subscript  $b$ ).  $\mathcal{S}_o$  and  $\mathcal{S}_b$  denote the single

layer integral for self-interaction for the outer boundary and the rigid body, respectively.  $\mathcal{S}_{ob}$  is the single layer integral due to the sources on the body at the target points on the outer boundary ( $\mathcal{S}_{bo}$  is defined similarly). There are double layer integral counterparts of these integrals as well. We can write the following equations

- The no-slip condition on the rigid body is

$$\frac{1}{2}\mathbf{v}(\mathbf{x}) + \mathcal{D}[\mathbf{v}](\mathbf{x}) = \mathcal{S}_b[\boldsymbol{\lambda}_b](\mathbf{x}) + \mathcal{S}_{bo}[\boldsymbol{\lambda}_o](\mathbf{x}) \quad (21)$$

- The balance of force and torque on the body is

$$\frac{1}{2}\mathcal{K}^*\boldsymbol{\lambda}_b + \mathcal{K}^*(\mathcal{D}_b^*[\boldsymbol{\lambda}_b] + \mathcal{D}_{bo}^*[\boldsymbol{\lambda}_o]) = \mathbf{F} \quad (22)$$

- The no-slip condition on the outer boundary is

$$\mathcal{S}_{ob}[\boldsymbol{\lambda}_b](\mathbf{x}) - \mathcal{D}_{ob}[\mathcal{K}\mathbf{U}](\mathbf{x}) + \mathcal{S}_o[\boldsymbol{\lambda}_o](\mathbf{x}) = \mathbf{0} \quad (23)$$

With this formulation, the linear system becomes

$$\begin{bmatrix} \mathcal{S}_b & -\frac{1}{2}\mathcal{K} - \mathcal{D}_b\mathcal{K} & \mathcal{S}_{bo} \\ -\frac{1}{2}\mathcal{K}^* - \mathcal{K}^*\mathcal{D}_b^* & \mathbf{0} & -\mathcal{K}^*\mathcal{D}_{bo}^* \\ \mathcal{S}_{ob} & -\mathcal{D}_{ob}\mathcal{K} & \mathcal{S}_o \end{bmatrix} \begin{bmatrix} \boldsymbol{\lambda}_b \\ \mathbf{U} \\ \boldsymbol{\lambda}_o \end{bmatrix} = \begin{bmatrix} \mathbf{u}_\infty \\ -\mathbf{F} \\ \mathbf{0} \end{bmatrix}. \quad (24)$$

This is again a symmetric linear system. Note that we implemented the decoupled and coupled formulations which give similar results up to 1E-4 error.

## 2.4. Suspensions

When there are multiple bodies in a flow, they induce flow on to each other. That adjusts the net flow on the bodies. These changes can be seen below. Let's consider  $M$  rigid bodies in a free-space flow  $\mathbf{u}_\infty(\mathbf{x})$ . The no-slip condition on the  $p^{\text{th}}$  body is

$$\begin{aligned} \frac{1}{2}\mathcal{K}[\mathbf{U}_p](\mathbf{x}) + \mathcal{D}_p[\mathcal{K}[\mathbf{U}_p]](\mathbf{x}) \\ = \mathbf{u}_\infty(\mathbf{x}) + \mathcal{S}_p[\boldsymbol{\lambda}_p](\mathbf{x}) \\ + \sum_{\substack{q=1 \\ q \neq p}}^M (\mathcal{S}_{pq}[\boldsymbol{\lambda}_q](\mathbf{x}) \\ - \mathcal{D}_{pq}[\mathcal{K}[\mathbf{U}_q]](\mathbf{x})). \end{aligned} \quad (25)$$

Here, the subscript  $(pq)$  denotes the hydrodynamic interaction between the  $p^{\text{th}}$  and  $q^{\text{th}}$  bodies. Then, the force-torque balance on the  $p^{\text{th}}$  body is

$$\frac{1}{2}\mathcal{K}_p^*\boldsymbol{\lambda}_p + \mathcal{K}^* \left( \mathcal{D}_p^*[\boldsymbol{\lambda}_p] + \sum_{\substack{q=1 \\ q \neq p}}^M \mathcal{D}_{pq}^*[\boldsymbol{\lambda}_q] \right) = \mathbf{F}_p. \quad (26)$$

## 2.5. Discretization

Since the single layer integral has a logarithmic singularity, we use the hybrid Gauss-trapezoid quadrature rule [21]. The double layer integral has no singularity in two dimensions. Therefore, the trapezoid rule is used. Let  $H$  be a diagonal matrix storing the quadrature weights, i.e.,  $H = \text{diag}(h)$ . Hence, the single layer integral can be discretized as

$$\mathcal{S}\boldsymbol{\lambda} \approx SH\boldsymbol{\lambda} = S(H\boldsymbol{\lambda}) \quad (27)$$

Note that the operator  $SH$  is not symmetric ( $(SH)^T = HS \neq SH$ ). However, the operator  $S$  acting on the discrete traction  $H\boldsymbol{\lambda}$  is symmetric. The geometric matrices can be discretized as

$$\mathcal{K}\mathbf{U} \approx K\mathbf{U} \quad (28)$$

$$\mathcal{K}^*\boldsymbol{\lambda} \approx K^T H\boldsymbol{\lambda} = K^T (H\boldsymbol{\lambda}) \quad (29)$$

Similarly, we can maintain the symmetry by using the discretized traction  $H\boldsymbol{\lambda}$  instead of the traction itself. Finally, the double layer operator is discretized as follows

$$\mathcal{D}\mathcal{K}\mathbf{U} \approx DHK\mathbf{U} \quad (30)$$

$$\mathcal{K}^*\mathcal{D}^*\boldsymbol{\lambda} \approx K^T HD^T H\boldsymbol{\lambda} = K^T HD^T (H\boldsymbol{\lambda}). \quad (31)$$

Let  $\mathbf{g} = H\boldsymbol{\lambda}$ , the linear system for the first alternative of the second kind formulation in the discrete form is

$$\begin{bmatrix} S & -\frac{1}{2}K - DHK \\ -\frac{1}{2}K^T - \frac{1}{2}K^T HD^T & 0 \end{bmatrix} \begin{bmatrix} \mathbf{g} \\ \mathbf{U} \end{bmatrix} = \begin{bmatrix} \mathbf{u}_\infty \\ -\mathbf{F} \end{bmatrix} \quad (32)$$

The discrete form for the confined flow is

$$\begin{bmatrix} S_b & -\frac{1}{2}K - D_bHK & S_{bo} \\ -\frac{1}{2}K^* - K^*HD_b^* & 0 & -K^*HD_{bo}^* \\ S_{ob} & -D_{ob}HK & S_o \end{bmatrix} \begin{bmatrix} \mathbf{g}_b \\ \mathbf{U} \\ \mathbf{g}_o \end{bmatrix} = \begin{bmatrix} \mathbf{u}_\infty \\ -\mathbf{F} \\ \mathbf{0} \end{bmatrix} \quad (33)$$

### 3. Results and Discussion

First, we will present the validation results of the numerical scheme. Then, we will compare the formulations for (i) single disk in a circular confinement, (ii) two disks pushed towards each other, (iii) suspension in a shear flow.

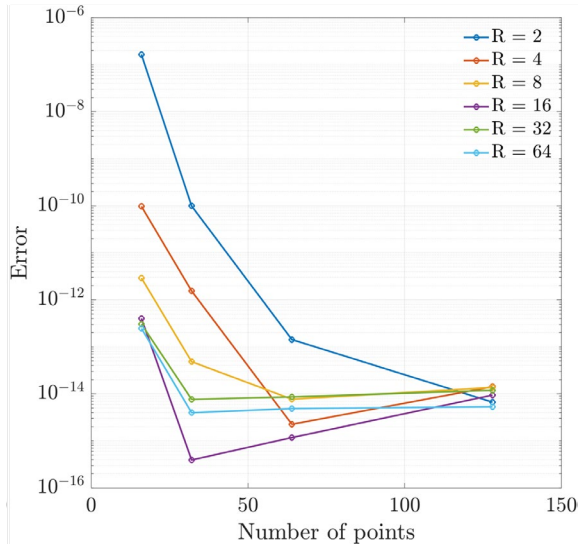


**Figure 1.** Validation results for the translational mobility test performed with the symmetric Alpert’s quadrature implementation. As the number of points increases, the error decreases as expected. Besides, the error is much less for larger confinements since the confinement effects decrease in larger confinements

#### 3.1. Validation

In our first test, we put a circular body of unit radius into a circular confinement of radius  $R$ . We set the fluid viscosity to unity as well. We apply a unit force in the  $x$ -direction for the translational mobility test and a unit torque for

the rotational mobility test. We discretized the body with  $N = [16, 32, 64, 128]$  points. We performed simulations for  $R = [2, 4, 8, 16, 32, 64]$ . For a chosen  $N$ , we made sure that the arc-length spacing is the same for the body and the confinement as we changed the confinement radius. We tested our scheme against the analytical results. The analytical translational velocity in the  $x$ -direction due to a force  $f_x$  in the same direction is

$$u_x = -\frac{f_x}{4\pi\eta h}$$

where the geometry related coefficient  $h$  is

$$h = \frac{R_1^2 + R_2^2}{R_1^2(\log R_2 + 1) + R_2^2(\log R_2) - R_2^2 - (R_1^2 + R_2^2)\log R_1}$$

with  $R_1$  is the radius of the disk (it is unity) inside the circular confinement of radius  $R_2$ . The results of the translational mobility test are in Figure 1. The analytical rotational velocity  $\omega$  due to a torque  $\tau$  is

$$\omega = \frac{\tau}{4\pi\eta} \frac{R_2^2 - R_1^2}{R_1^2 R_2^2}$$

The validation results of the rotational mobility test are in Figure 2. In both tests, the error is the relative error in the translational (or rotational) velocity given the force (or torque). The results show that the error exponentially decreases to the machine precision as the number of points to discretize the body increases.

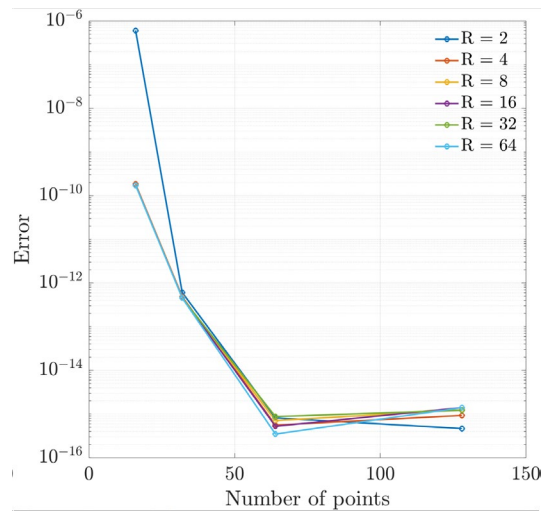


**Figure 2.** Validation results for the rotational mobility test

### 3.2. Comparison: Second kind vs. first kind

Here, we compare the second kind and the first kind formulations in various examples. We test how the number of GMRES iterations differs in the problems where (a) the disk is driven by a vertical force and (b) the disk is driven by the motion defined on a circular confinement.

In the first problem, we consider a disk of radius 0.5 in a circular confinement of radius 5. We ensure that the disk and the confinement have the same minimum arclength spacing while changing the number of points on the disk. The disk is initially off-centered at  $x = 0.5$ . The GMRES tolerance is set to  $1E-10$ . The results are in Table 1. In this test problem, both formulations lead to the same number of GMRES iterations when solving the linear system.

**Table 1.** Number of GMRES iterations required when solving the linear system with first and second kind formulations for a disk moving under a constant vertical force in a confinement

Number of points	First kind	Second kind
16	26	26
32	26	26
64	26	26
128	25	25

In the second problem, we consider a disk in a confinement on which a tangential velocity is defined. The results are in Table 2. While both formulations lead to the same number of GMRES iterations, this problem requires a smaller number of GMRES iterations than the case where the disk is moved with a force.

**Table 2.** Number of GMRES iterations required when solving the linear system with first and second kind formulations for a disk moving in a confinement on which tangential velocity is defined

Number of points	First kind	Second kind
16	19	19
32	19	19
64	20	20
128	21	21

Later, we test problems where there are two disks. In the first problem, we consider two disks driven towards each other by an external force in free space. The disks have the same radius of 0.5. One of them is at  $[-4, 0]$  and the other one is at

$[4, 0]$ . They are driven towards each other with force  $[1, 0]$  and  $[-1, 0]$ , respectively. The true physics involve two disks staying at a minimum distance in the equilibrium. The GMRES tolerance is  $1E-10$ . The results are in Tables 3 and 4 for the second and first kind formulations, respectively. The results show that the second kind formulation gives the converged solution with 32 points while the first kind formulation requires another step of refinement (convergence in the minimum distance between particles). In terms of the number of GMRES iterations, there are not major differences between both formulations.

**Table 3.** Number of GMRES iterations for the problem of two disks driven towards each other with external force solved with the second kind formulation

Number of points	Average GMRES	Maximum GMRES	Minimum distance
16	25	34	0.0782
32	29	53	0.0714
64	29	71	0.0714
128	26	88	0.0714

**Table 4.** Number of GMRES iterations for the problem of two disks driven towards each other with external force solved with the first kind formulation

Number of points	Average GMRES	Maximum GMRES	Minimum distance
16	25	34	0.0788
32	29	53	0.0715
64	29	69	0.0714
128	26	88	0.0714

**Table 5.** Number of GMRES iterations for the problem of two disks in a free-space shear flow solved with the second kind formulation

Number of points	Average GMRES	Maximum GMRES	Minimum distance
16	29	54	0.1315
32	29	75	0.1316
64	28	101	0.1316
128	27	46	0.1316

In the second problem with multiple disks, we place them in a free-space shear flow. One disk is at  $[-8, 0.25]$  and the other one is at  $[0, 0]$ . Hence, the disk on the left flows towards the disk at  $[0, 0]$  and passes over it. The results are tabulated in Tables 5 and 6 for the first and second kind formulations, respectively. The first

kind formulation requires a smaller number of maximum GMRES iterations at a step however the average GMRES iterations is similar in both cases.

**Table 6.** Number of GMRES iterations for the problem of two in a free-space shear flow solved with the first kind formulation

Number of points	Average GMRES	Maximum GMRES	Minimum distance
16	28	50	0.1310
32	28	59	0.1316
64	27	78	0.1316
128	27	46	0.1316

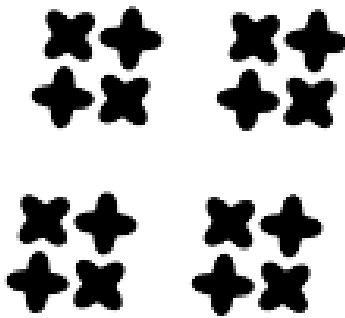


**Figure 3.** Suspension of 16 star-shaped disks in free-space shear flow

Finally, we put 16 disks in star-shape (Figure 3) in a free-space shear flow. They are discretized with  $N = 64$  points. We simulate this case for various values of the GMRES tolerance. Table 7 shows the number of GMRES iterations obtained in both formulations. While for large tolerances both formulations require similar numbers of GMRES iterations, for small GMRES tolerance the first kind formulation requires a smaller number of GMRES iterations, and hence is more preferred.

**Table 7.** Number of GMRES iterations required when solving the linear system with first and second kind formulations for 16 disks (discretized with 64 points) in free-space shear flow

GMRES tolerance	First kind	Second kind
1E-4	97	97
1E-6	120	120
1E-10	190	269

The second kind formulations are known to have better conditioning than the first kind formulations because of the presence of the double layer operator instead of the single layer operator in the formulation. The question is why the proposed symmetric second kind formulation gives similar numbers of GMRES iterations with the first kind formulation. Youngren & Acrivos [22] distinguishes the two formulations based on whether the double layer integral appears alone or with the single layer integral. If the double layer integral appears by itself, the problem is solved for an unknown (non-physical) density which is then postprocessed to find physical quantities such as traction and velocity. This kind of formulation is called the second kind formulation. If the single layer integral appears in the formulation, that formulation becomes the first kind. Since the single layer operator has unbounded condition number (whereas the double layer operator's condition number is bounded), the appearance of the single layer operator in our proposed formulation makes it first-kind.

To conclude the comparison, we compare the formulations so far with Power & Miranda's second kind formulation [18] in the case of 16 star-shaped disks in free-space shear flow (Figure 3). For the first kind formulation, the number of GMRES iterations is 191 without a preconditioner and 27 with the block-diagonal preconditioner [23]. For the proposed formulation here, the number of GMRES iterations is 269 without the preconditioner and 27 with the preconditioner. Finally, for the Power & Miranda's second kind formulation, the number of GMRES iterations is 111 without a preconditioner and 27 with the block-diagonal preconditioner. Overall, we suggest the first kind formulation for the simulations of Stokesian flows of rigid particles. The formulation is easy to implement and is symmetric. It results in similar stability and convergence properties as the Power & Miranda's second kind formulation and the second kind formulation proposed in this article.

#### 4. Conclusion

In this article, we presented a detailed comparison of the first kind and second kind integral equation formulations for the Stokesian particulate flows in two dimensions in terms of stability, accuracy and performance. To the best of our knowledge, this is one of the first comparative studies of these different formulations. We first aimed at developing a symmetric positive definite second kind formulation that can be used to simulate active particles with Brownian motion. This formulation inherently included the single-layer integral operator that causes the formulation to have similar stability properties as the first kind formulation. Hence, the first kind formulation must still be preferred over the proposed second kind formulation. After comparing these two formulations with the Power & Miranda's second kind formulation, we found out that the first kind formulation does not have much worse stability properties than the second kind formulation. Hence, we conclude that the first kind formulation provides efficient means to simulate active particles in their Stokesian flows.

#### Article Information Form

##### *Acknowledgments*

The author would like to thank Floren Balboa for the idea and help with the analytical calculations.

##### *Funding*

The author has not received any financial support for the research, authorship or publication of this study.

##### *Author Contribution*

Conceptualization, Methodology, Software, Data curation, Visualization, Investigation, Writing and Editing.

##### *The Declaration of Conflict of Interest/ Common Interest*

No conflict of interest or common interest has been declared by the author.

##### *The Declaration of Ethics Committee Approval*

This study does not require ethics committee permission or any special permission.

##### *The Declaration of Research and Publication Ethics*

The author of the paper declares that they comply with the scientific, ethical and quotation rules of SAUJS in all processes of the paper and that they do not make any falsification on the data collected. In addition, they declare that Sakarya University Journal of Science and its editorial board have no responsibility for any ethical violations that may be encountered, and that this study has not been evaluated in any academic publication environment other than Sakarya University Journal of Science.

##### *Copyright Statement*

The author owns the copyright of their work published in the journal and their work is published under the CC BY-NC 4.0 license.

#### References

- [1] E. Lauga, T. R. Powers, "The hydrodynamics of swimming microorganisms," *Rep. Prog. Phys.* 72, 096601, 2009.
- [2] J. Happel, H. Brenner, "Low Reynolds Number Hydrodynamics: With Special Applications to Particulate Media," Springer, Berlin, 2012.
- [3] D. Barthes-Biesel, "Microhydrodynamics and Complex Fluids," CRC, Boca Raton, FL, 2012.
- [4] J. Palacci, S. Sacanna, A. P. Steinberg, D. J. Pine, P. M. Chaikin, "Living crystals of light-activated colloidal surfers," *Science* 339 (6122), 2013, pp.936-940.
- [5] W. F. Paxton, K. C. Kistler, C. C. Olmeda, A. Sen, S. K. St. Angelo, Y. Cao, T. E. Mallouk, P. E. Lammert, V. H. Crespi, "Catalytic Nanomotors: Autonomous Movement of Striped Nanorods," *Journal of the American Chemical Society* 126(41), 2004, pp.13424-13431.
- [6] J. R. Howse, R. A. L. Jones, A. J. Ryan, T. Gough, R. Vafabakhsh, R. Golestanian, "Self-Motile Colloidal Particles: From Directed Propulsion to Random Walk,"

- Physical Review Letters 99(4), 2007, pp.48102.
- [7] S. J. Ebbens, J. R. Howse, "In pursuit of propulsion at the nanoscale," *Soft Matter* 6(4), 2010, pp.726-738.
- [8] S. Ghose, R. Adhikari, "Irreducible representations of oscillatory and swirling flows in active soft matter," *Physical Review Letters*. 112, 2014, pp.118102.
- [9] B. Delmotte, E. E. Keaveny, F. Plouraboue, E. Climent, "Large-scale simulation of steady and time-dependent active suspensions with the force-coupling method," *Journal of Computational Physics*. 302, 2015, pp.524-547.
- [10] A. Pandey, P. B. S. Kumar, R. Adhikari, "Flow-induced nonequilibrium self-assembly in suspensions of stiff, apolar, active filaments," *Soft Matter* 12, 2016, pp.9068-9076.
- [11] D. Lindbo, A-K. Tornberg, "Spectrally accurate fast summation for periodic Stokes potentials," *Journal of Computational Physics*. 229(23), 2010, pp.8994-9010.
- [12] S. Kim, S. J. Karrila, "Microhydrodynamics: Principles and selected applications," Courier Corporation, 2013.
- [13] C. Pozrikidis, "Boundary integral and singularity methods for linearized viscous flow," Cambridge University Press, 1992.
- [14] A-K. Tornberg, L. Greengard, "A fast multipole method for the three-dimensional Stokes equations," *Journal of Computational Physics*. 227(3), 2008, pp.1613-1619.
- [15] M. Rachh, L. Greengards, "Integral equation methods for elastance and mobility problems in two dimensions," *SIAM Journal on Numerical Analysis* 54(5), 2016, pp.2889-2909.
- [16] E. Corona, L. Greengards, M. Rachh, S. Veerapaneni, "An integral equation formulation for rigid bodies in Stokes flow in three dimensions," *Journal of Computational Physics*. 332, 2017, pp.504-519.
- [17] D. J. Smith, "A boundary element regularized Stokeslet method applied to cilia-and-flagella-driven flow," *Proceed. of the Royal Society of London A* 465(2112), 2009, pp.3605-3626.
- [18] H. Power, G. Miranda, "Second Kind Integral Equation Formulation of Stokes' Flows Past a Particle of Arbitrary Shape," *SIAM Journal on Applied Mathematics* 47(4), 1987, pp.689-698.
- [19] G. Kabacacoglu, B. Quaipe, G. Biros, "Low-resolution simulations of vesicle suspensions in 2D," *Journal of Computational Physics*. 357(43), 2018, pp.43-77.
- [20] E. Corona, S. Veerapaneni, "Boundary integral equation analysis for suspension of spheres in Stokes flow," *Journal of Computational Physics*. 362, 2018, pp.327-345.
- [21] B. K. Alpert, "Hybrid Gauss-trapezoidal quadrature rules," *SIAM Journal of Scientific Computing*. 20, 1999, pp.1551-1584.
- [22] G. K. Youngren, A. Acrivos, "Stokes flow past a particle of arbitrary shape: a numerical method of solution," *Journal of Fluid Mechanics* 69(2), 1975, pp.377-403.
- [23] A. Rahimian, S. K. Veerapaneni, G. Biros, "Dynamic simulation of locally inextensible vesicles suspended in an arbitrary two-dimensional domain, a boundary integral method," *Journal of Computational Physics*. 229, 2010, pp.6466-6484.